# Divergence time and environmental similarity predict the strength of morphological convergence in stick and leaf insects

Romain P. Boisseau[1,2*], Sven Bradler[3], Douglas J. Emlen[1]

[1]Division of Biological Sciences, University of Montana, Missoula, MT, United States of America;
[2]Department of Ecology and Evolution, University of Lausanne, Lausanne, Switzerland;
[3]Department of Animal Evolution and Biodiversity, Johann-Friedrich-Blumenbach Institute of Zoology and Anthropology, University of Göttingen, Göttingen, Germany

*Corresponding authors: Romain P. Boisseau and Douglas J. Emlen

**Email**: romain.boisseau@unil.ch, doug.emlen@mso.umt.edu

**Author Contributions:** R.P.B., S.B. and D.J.E. designed research; S. B. curated and contributed specimens; R.P.B. performed the research; R.P.B. analyzed the data; R.P.B. and D.J.E. wrote the paper.

The authors declare that they have no conflicts of interest.

All data and code used in this study will be made available in a public repository (figshare).

**Classification**: Biological Sciences, Evolution

**Keywords**: Phasmatodea | ecomorph | homoplasy | macroevolution | repeated evolution

This file includes:

Main Text

Figures 1 to 6

**Abstract**

Independent evolution of similar traits in lineages inhabiting similar environments (convergent or repeated evolution) is often taken as evidence for adaptation by natural selection, and used to illustrate the predictability of evolution. Yet convergence is rarely perfect for two reasons. First, environments may not be as similar as they appear. Second, responses to selection are contingent upon available genetic variation and independent lineages may differ in the alleles, genetic backgrounds, and even the developmental mechanisms responsible for the phenotypes in question. Both impediments to convergence are predicted to increase as the length of time separating two lineages increases, making it difficult to discern their relative importance. We quantified environmental similarity and the extent of convergence to show how habitat and divergence time each contribute to observed patterns of morphological evolution in 212 species of stick and leaf insects (order Phasmatodea). Dozens of phasmid lineages independently colonized similar habitats, repeatedly evolving in parallel directions on a 23-trait morphospace, though the magnitude and direction of these shifts varied. Lineages converging towards more similar environments ended up closer on the morphospace, as did closely related lineages, and closely related lineages followed more parallel evolutionary trajectories to arrive there than more distantly related ones. Remarkably, after accounting for habitat similarity, we show that divergence time reduced the extent of convergence at a constant rate across more than 100 million years of separation, suggesting even the magnitude of contingency can be predictable, given sufficient spans of time.

**Significance statement**

Phasmids (stick and leaf insects) exemplify the extraordinary power of natural selection to shape organismal phenotypes. The animals themselves are charismatic champions of crypsis and masquerade; and our characterization of their adaptive radiation reveals dozens of instances

of convergence, as lineages adapted to similar changes in habitat by repeatedly evolving similar body forms. Our findings show that the similarity of environmental conditions experienced by the organisms – the closeness of the invaded niches – and the extent of elapsed time since divergence, both predict the strength of morphological convergence. The phasmid radiation reveals an evolutionary process that is surprisingly predictable, even when lineages have been evolving independently for tens of millions of years.

## Introduction

When does convergent evolution happen? Examples of lineages independently evolving similar phenotypes are numerous and conspicuous (also referred to as 'repeated evolution') (1–5) (e.g., gliding mammals (6), cave amphipods (7, 8), Hawaiian spiders (9)), and likely result from adaptation to similar ecological niches (3, 9, 10, but see 11). Yet convergence is rarely perfect and sometimes does not occur at all, even when habitats are similar. When it does occur, the extent of phenotypic similarity varies widely (6, 10, 13) and the factors causing this variation and, by extension, influencing the repeatability of evolutionary outcomes, are not well understood (14, 15).

One important determinant of the likelihood and extent of convergent evolution is the degree of relatedness among lineages. Repeated evolution usually involves closely related taxa (11) (e.g., Caribbean *Anolis* lizards (16, 17), three-spined stickleback fish (18)), suggesting that strong convergence is most likely when the time separating lineages is brief (i.e., phylogenetic bias (15)). Gould famously argued that evolutionary outcomes are contingent on the intricate series of historical events uniquely experienced by each lineage (19–21). Closely related lineages share more of their evolutionary history and, consequently, more of their genetic variation (18, 22–27). They are also more likely to share the same ancestral niche and associated ancestral phenotypes (14). Threespine stickleback repeatedly colonized lakes and streams from the same marine habitat, for example (22, 28). In these instances, adaptation to

the new niche is likely to proceed through similar sequences of phenotypic changes (i.e., parallel or collinear evolutionary trajectories (5)) arriving at phenotypes that are strongly resemblant. More disparate lineages may approach a shared environmental challenge from different starting phenotypes, with weaker convergence as a result. And lineages with enough accumulated differences may not converge at all. Aye-ayes (Primates) and woodpeckers (Aves) each catch and eat insect larvae found under the bark of trees, yet they forage in strikingly different ways (14). Aye-ayes use their teeth to break through the bark and an elongated middle finger to catch larvae, while woodpeckers use hammering beaks to get through the bark and long, barbed tongues to catch insects.

Consequently, the extent of shared evolutionary history and the similarity of phenotypic ancestral states should each affect the likelihood of repeated phenotypic evolution. Specifically, the lower the opportunity for contingency – less accumulated time since their split – the more likely any two lineages should be to converge strongly in response to a shared selection environment. A 2015 meta-analysis supported this prediction: convergent evolution was more likely to be documented among closely related than distantly related taxa, particularly when considering morphology (11). This pattern also holds at the molecular level, as the degree of gene reuse decreases with divergence time when lineages repeatedly adapt to similar environments (24–27, 29), or evolve analogous individual traits (23). Yet explicit tests of Gould's predicted link between divergence time and the extent of phenotypic convergence are lacking.

Quantifying the role of divergence time on convergence requires a system (i) where the extent of phenotypic convergence and environmental similarity can be quantified precisely; (ii) where instances of convergence span vast periods of time from recently diverged to much more distantly genetically related lineages; and (iii) where there are enough instances of convergence to allow sufficient statistical power. Here, we use the morphological diversity of stick and leaf

105 insects (order Phasmatodea, ~3,500 described species) to provide such test. Most species
106 exhibit stunning forms of camouflage through background matching (crypsis (30)) and the
107 mimicry of objects irrelevant to predators (masquerade (31)) such as sticks, leaves, bark pieces,
108 or moss (32–34). Selection to match such diverse objects produced a spectacular morphological
109 diversity ranging from elongated tubular bodies with long slender legs to bodies so wide and
110 flattened they look like leaves (Fig. 1). Recent phylogenetic studies of phasmids conflict with
111 prior taxonomic classifications based on morphological characters, suggesting a high degree of
112 morphological convergence across the Phasmatodea (35–39). For example, the "tree lobsters"
113 – flightless, robust and strongly armored species, including the famous Lord Howe Island stick
114 insect—had been grouped into the subfamily Eurycanthinae but were later shown to be highly
115 polyphyletic, illustrating a dramatic case of morphological convergence (35)(Fig. 1 O,P).
116 Moreover, several authors have suggested that apterous, stockier, spinier, and darker body
117 forms tend to be found close to the ground, while more elongated and winged forms tend to rest
118 higher up in the vegetation, implicating a role of ecological niche in driving these convergent
119 patterns (33, 40).

120 We quantitatively assessed the presence and extent of convergent evolution in body
121 morphology in stick insects using a time-calibrated multilocus phylogeny of the order and an
122 associated morphospace of female body morphology. Our analyses identified 21 distinct body
123 types (ecomorphs), many described here for the first time, and revealed dozens of instances of
124 morphological convergence. These repeated invasions of restricted and distinct portions of the
125 morphospace were associated with behavioral transitions towards similar habitat uses. Using
126 the independent transitions to resting on the leaf litter and trunks (n=1), and to resting on leaves
127 and branches (n=16), we then examined how divergence time, ancestral habitat use, and
128 environmental distance affected the extent of morphological convergence.

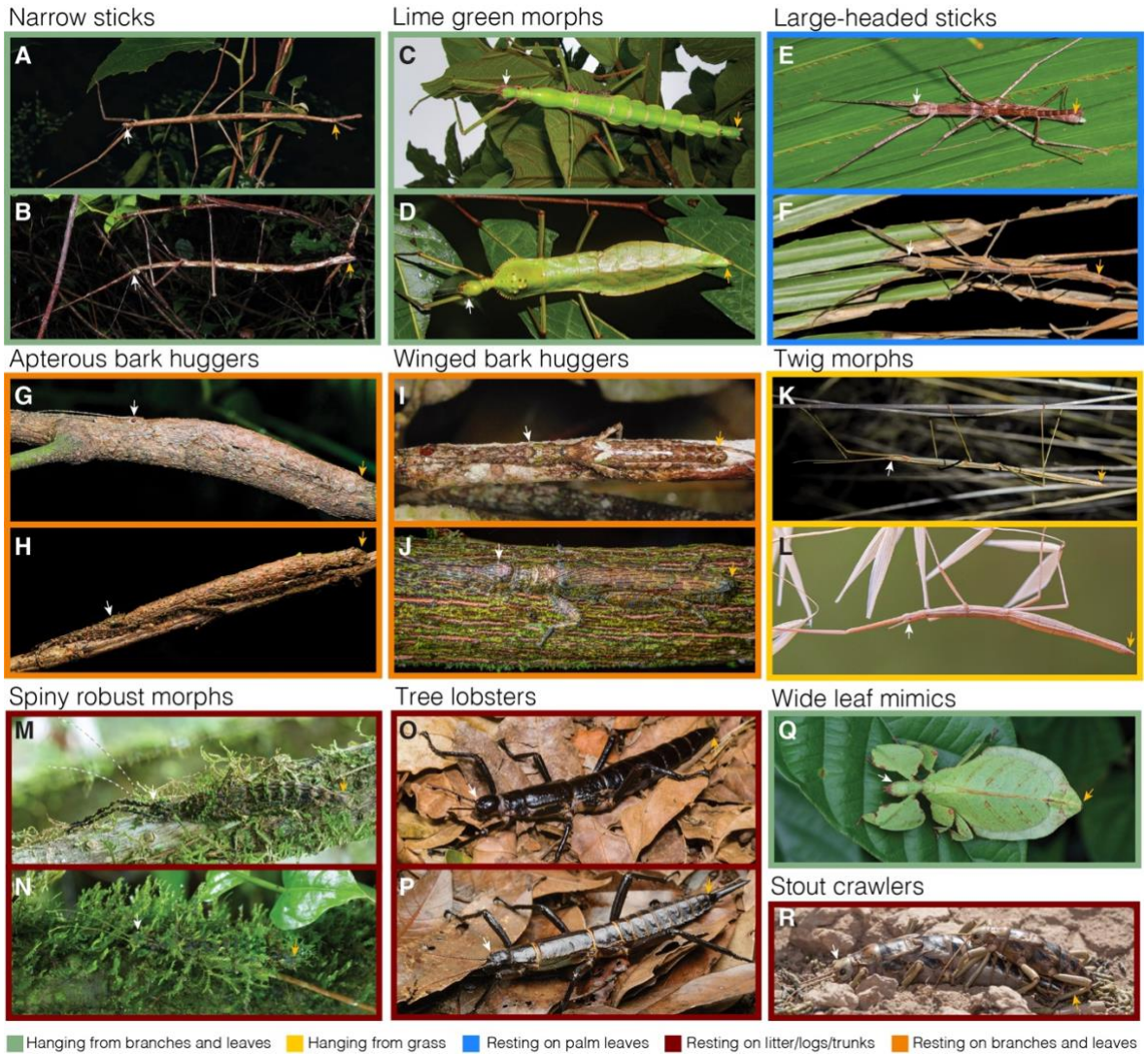


**Figure 1: Photographs of adult females *in situ*.** The color surrounding each picture corresponds to a habitat use category. White arrows point to the head, orange arrows point to the end of the abdomen of the specimens. Pictures included under the same ecomorph name represent cases of convergent evolution (i.e., unrelated lineages). **A,** *Ctenomorpha marginipennis* (Australia, Lanceocercata) (CC-BY-NC 4.0 Julie Graham, inaturalist.org/observations/73831515); **B,** *Phobaeticus kirbyi* (Malaysia, Pharnaciini) (CC-BY-SA 2.0 Bernard Dupont, flickr.com). **C,** *Monandroptera acanthomera* (Réunion, Lanceocercata) (© Nicolas Cliquennois, used by permission); **D,** *Cranidium gibbosum* (French Guiana, Diapheromerinae) (CC-BY-NC 4.0 Sébastien Sant, inaturalist.org/observations/75953936). **E,** *Apterograeffea reunionensis* (Réunion, Lanceocercata) (© Nicolas Cliquennois, used by permission); **F,** *Graeffea crouanii* (French Polynesia, Lanceocercata) (CC-BY-NC 4.0 Tahiticrabs, inaturalist.org/observations/165663078). **G,** *Leosthenes aquatilis* (New Caledonia, Lanceocercata) (CC-BY-NC 4.0 Damien Brouste, inaturalist.org/observations/24180348); **H,** *Pseudoleosthenes irregularis* (Madagascar, African/Malagasy clade) (© Paul Bertner, used by permission). **I,** *Epicharmus marchali* (Mauritius, Lanceocercata) (© Sylvain Hugel and Nicolas Cliquennois, used by permission); **J,** *Prisopus berosus* (Belize, Pseudophasmatinae) (CC-BY-NC 4.0 Thomas Shahan, inaturalist.org/observations/50919578). **K,** *Denhama sp.* (Australia, Lonchodinae) (CC-BY-NC 4.0 Enot Poluskuns, inaturalist.org/observations/166373254); **L,** *Clonopsis gallica* (Spain, European clade) (CC-BY 2.0 Ramón Portellano, flickr.com). **M,** *Parectatosoma sp.* (Madagascar, African/Malagasy clade) (© Paul Bertner, used by permission); **N,** *Taraxippus samarae* (Panama, Cladomorphinae) (© Paul Bertner, used by permission, inaturalist.org/observations/19995010). **O**, *Dryococelus australis* (Australia, Lanceocercata) (© Angus McNab, used by permission); **P**, *Eurycantha immunis* (Papua, Indonesia, Lonchodinae) (© Chien C. Lee, used by permission). **Q**, *Pulchriphyllium bioculatum* (Singapour, Phylliidae) (CC-BY-NC 4.0, Catalina Tong, inaturalist.org/observations/154447000); **R**, *Agathemera crassa* (Chile, Pseudophasmatinae) (CC-BY-NC-SA 4.0 Ariel Cabrera Foix, inaturalist.org/observations/29411794).

# Results

**Repeated evolution of ecomorphs in Phasmatodea.** To reconstruct the evolutionary history of Phasmatodea, we used genetic data from three nuclear and four mitochondrial genes across 314 phasmid taxa, and applied Bayesian inferences with six unambiguous crown-group phasmid fossils as minimum calibration points (Table S1). The relationships between the major euphasmatodean clades that arose during an ancient radiation were constrained to match the basal topology inferred in previous phylotranscriptomic studies (37, 41). The inferred Maximum Clade Credibility (MCC) tree was overall strongly supported and was largely congruent with previous studies (Fig. 2)(36, 39, 42), providing a robust framework for all subsequent comparative analyses. 16 major clades were recovered and appeared largely defined by geographic distribution and ecozones (Fig. 2). The split between Embioptera and Phasmatodea is estimated to have occurred 125 million years ago (mya) [95% Highest Posterior Density (HPD): 122 – 130mya] and between Timematidae and Euphasmatodea to 102mya [95% HPD: 99 – 108mya].

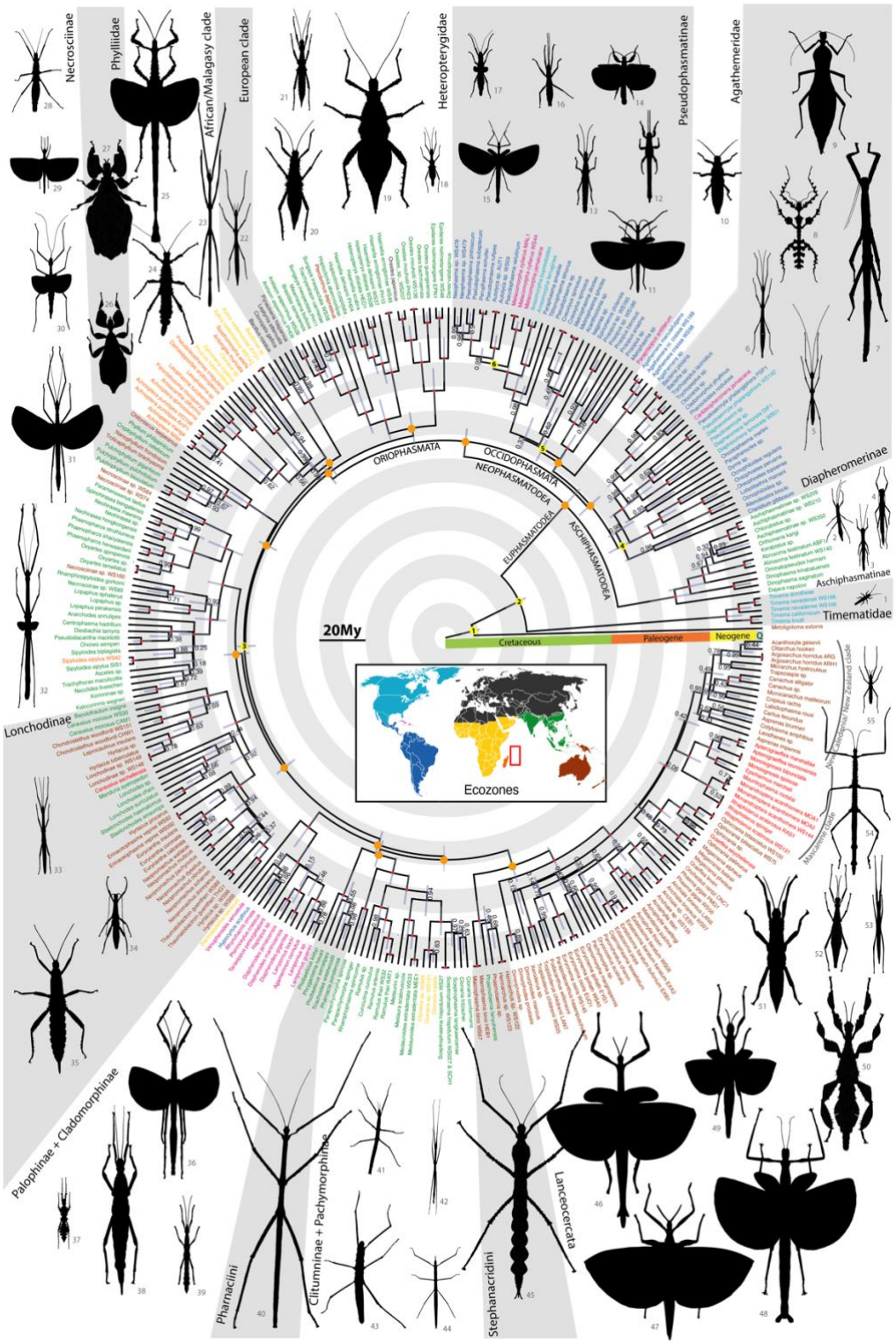


**Figure 2: Time-calibrated maximum clade credibility tree and geographic distribution of stick and leaf insects.** Fossil calibration points are denoted with numbered yellow circles (Table S1). Orange circles correspond to constrained nodes based on the topology inferred from transcriptomes of Tihelka et al. (41). 95% confidence intervals around node ages are indicated by gray bars and Bayesian posterior probabilities are indicated at each node. Red nodes represent fully supported nodes with posterior probabilities equal to one. Tip labels are colored by ecozone following the colors of the central inset. The red rectangle on the world map indicates islands of the Mascarene plateau. Scaled adult female silhouettes were drawn by the first author and correspond to the species listed in Table S2.

We assembled a morphological dataset comprising 1359 adult female specimens from 212 species included in the phylogeny and including 21 quantitative size-controlled measurements (i.e., phylogenetic residuals against body volume) and qualitative data on cuticle texture of the thorax and abdomen (i.e., spiny/rough versus smooth) (Fig. S1). From this dataset, we reconstructed a size-controlled multidimensional morphospace using a mixed Principal Component Analysis (PCAmix)(43). PCAmix combines a principal component analysis (PCA) with a multiple correspondence analysis (MCA), allowing the inclusion of both numerical and categorical variables. This analysis revealed large variation between phasmid species in relative body width (PC1, 50.7% of the total variation), relative wing size (PC2, 11.5%), relative body height (i.e., how flattened the body is; PC3, 9.8%), body texture (i.e., how smooth or rough the body cuticle is; PC4, 7.0%) and relative head size (PC5, 5.3%) (Fig. 3A-B, S2). The first five PCs together accounted for 84.4% of the total variation. The clade Phylliidae (i.e., true leaf insects) stands out from the rest of the phasmids on the morphospace (dark green in Fig. 3A-B) as phylliids are characterized by an exceptionally widened and flat abdomen giving them the appearance of wide angiosperm leaves (Fig. 1Q) (44). Other phasmid clades appeared more centered on the morphospace, varying mostly in relative body width ranging from extremely elongated to more robust body silhouettes (Fig. 3A-B). Species with extreme morphologies were scattered at the periphery of this central core, often only projecting out along a single axis. For instance, the large-headed palm stick insects (subfamily Megacraniinae) mostly stand out along the PC5 axis that separates species based on relative head size (Fig. 1 E,F, Table S3). Most of the morphological diversity is found in the Euphasmatodea, consistent with their much greater species diversity (n>3400 species), compared to Timematodea (n=21 species), which is morphologically homogeneous (Fig. 3C). The reconstructed morphological diversification of Euphasmatodea can be visualized in Video S1.

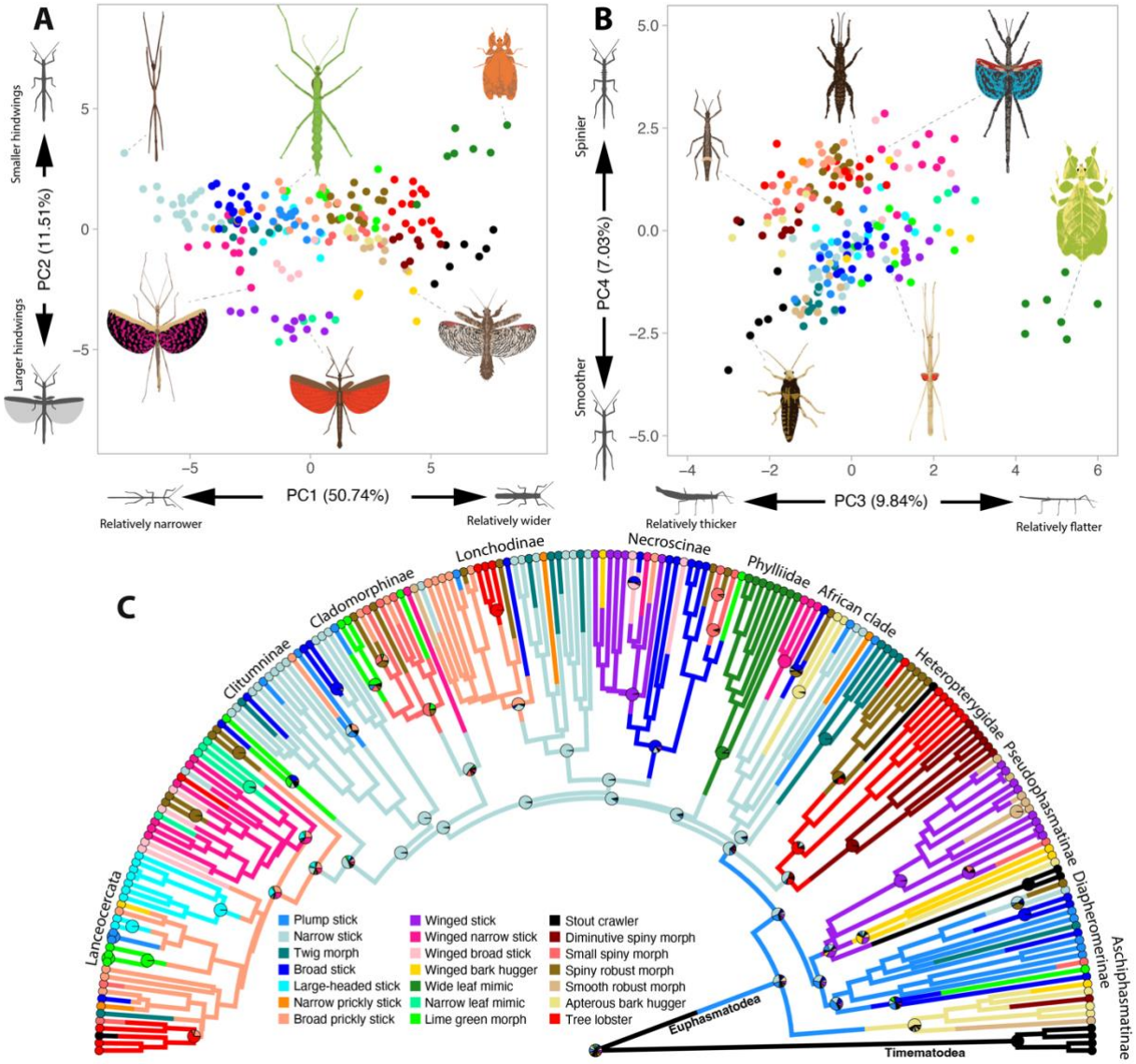


**Figure 3: Repeated ecomorphological evolution in stick and leaf insects. A-B:** Morphospace (first four dimensions) with species colored by assigned ecomorph (see fig. 4). **C**: Ancestral state reconstruction of ecomorphs using stochastic character mapping. The pie charts at nodes represent the posterior probabilities that each internal node is in each state. The color legend applies to all panels.

We then used an agglomerative hierarchical clustering approach to define and assign species to clusters occupying relatively distinct regions of the multidimensional morphospace (Fig. 3A-B, 4, S3-5)(7, 8, 45). The optimum number of clusters (k=21) was determined using the biological homogeneity index [BHI, (46)] to maximize the homogeneity of habitat use within each cluster (Fig. S6). BHI measures the average proportion of taxon pairs with similar habitat uses and which are clustered together morphologically. For 21 clusters, BHI was 0.81, which highlights the strong association between habitat use and the defined morphological

clusters, thereafter referred to as ecomorphs following the definition by Williams (i.e., species with a similar habitat, morphology and behavior, but not necessarily closely related)(47). As expected, among the 21 ecomorphs, we recovered the *wide leaf mimic* ecomorph (only comprising the Phyllidae clade, Fig. 1Q) and the previously recognized *tree lobster* ecomorph (Fig. 1 O,P), which includes the thorny devil stick insects (*Eurycantha* spp.) and the Lord Howe Island stick insects (*Dryococelus australis*)(35). Using random forest machine learning models (48), we identified the main morphospace axes that were most helpful for these predictive models to infer ecomorph from the morphological data and therefore the axes best distinguishing each ecomorph (Table S3). This analysis revealed that ecomorphs are often distinguished by only a few dimensions of the morphospace. For instance, *spiny robust morphs* were best distinguished by PC1 (i.e., relative body width) and PC4 (i.e., body texture) due to their stocky and rough or spiny bodies, often mimicking bark pieces or moss (Fig. 1 M,N; Table S3, Fig. S4).

A discrete ancestral state reconstruction based on stochastic character mapping (49–51) suggested that the *wide leaf mimic* ecomorph (clade Phyllidae, Fig. 1Q) was the only one with a unique origin (Fig. 3C, Table S3). All other ecomorphs appeared to have originated at least twice (e.g., *Diminutive spiny morph*) and up to at least 10 times (e.g. *broad stick* ecomorph), indicating widespread morphological convergence in the order (Fig. 3C).

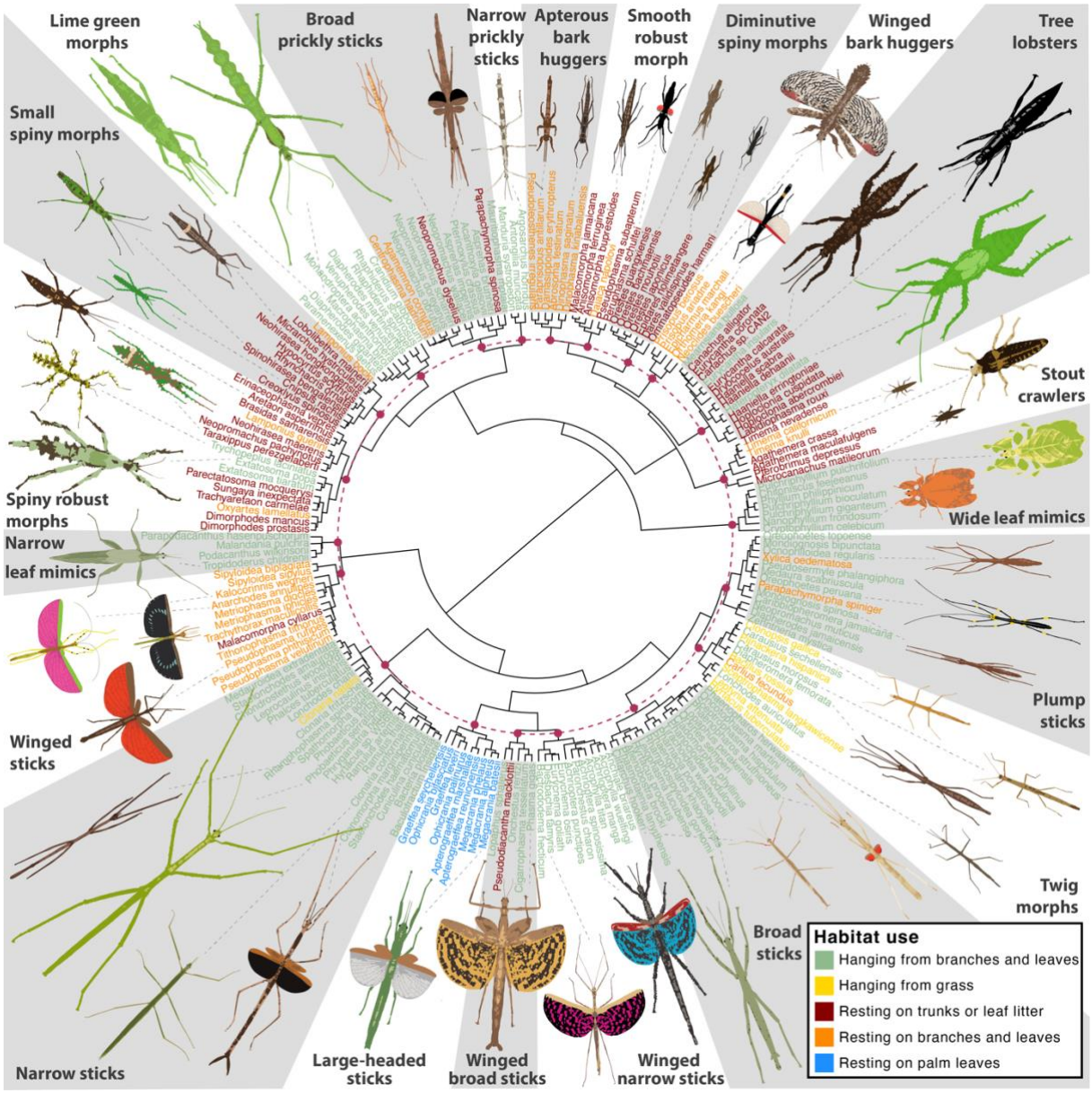


**Figure 4: Phenogram of overall morphological similarity across adult female phasmids.** Hierarchical cluster dendrogram based on 21 continuous and 2 discrete morphological variables using the Ward's method. Tip labels are colored according to extant habitat use. The dashed maroon circle corresponds to the height threshold used to delineate ecomorphs. Intersection between the circle and dendrogram branches are shown as maroon dots. Scaled adult female illustrations correspond to the taxon indicated with a dashed grey line.

**Phasmid morphology and habitat use are closely associated.** A stochastic character mapping of habitat use reconstructed the ancestor of all phasmatodeans as most likely having rested on the leaf litter, trunks, or logs during the day (Fig. 5A). However, the ancestors of most euphasmatodean clades were inferred as hanging from branches and leaves (Fig. 5A). Overall, this reconstruction indicated between 15 and 19 secondary transitions to resting on the leaf

249 litter, logs and trunks, 18 transitions to resting on branches and leaves, five to hanging from
250 grass, and two to resting on palm leaves (Fig. 5A). We calculated the size of the
251 multidimensional hypervolumes occupied by each habitat category on the morphospace using
252 range boxes and kernel density estimates (52, 53). Species hanging from branches occupied the
253 largest volume on the morphospace, species hanging from grass or resting on palm leaves the
254 smallest (Fig. 5B-C, S7-8). This reflects the considerable variation in body morphology of
255 species hanging from branches going from extremely elongated and cylindrical stick-like
256 species (e.g., Fig. 1 A,B) to wide and flat leaf-like species (e.g., Fig. 1 Q). Hypervolume
257 overlap, as measured by different methods, was overall relatively low between habitat
258 categories (Jaccard similarity ranged from 0 to 0.17, Sorensen similarity from 0 to 0.29) (Fig.
259 S9-10). Random forest models (i.e., machine learning classification algorithms) reached 84.3%
260 accuracy when classifying the habitat use of taxa based solely on morphospace coordinates
261 (Fig. 5D-E). The accuracy of predictions was limited when only based on the first morphospace
262 axis, despite PC1 accounting for more than half of the phenotypic variance (50.7%, Fig. S2),
263 but plateaued after including the first 5 axes only (Fig. 5E). Clades varied widely in their
264 occupied hypervolume: clades displaying diverse habitat uses (e.g., Lanceocercata, African
265 clade) occupied the largest volumes on the morphospace while clades displaying largely
266 uniform habitat uses (e.g., Phyllidae, Heteropterygidae) occupied restricted volumes (Figure
267 5A, S11).
268
269
270
271

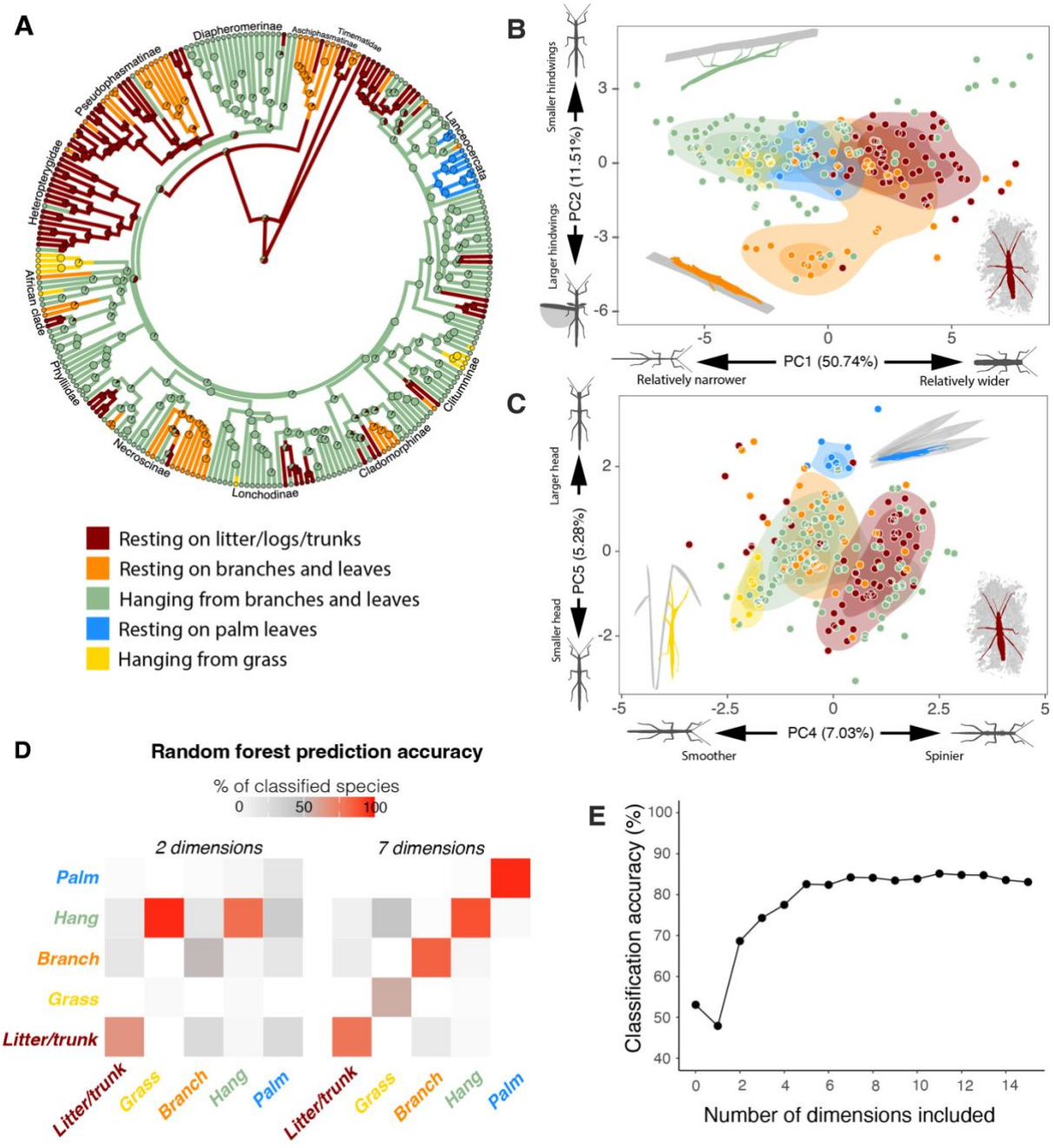


**Figure 5: Habitat transitions and morphospace occupation and overlap between different habitats. A:** Ancestral state reconstruction of habitat use using stochastic character mapping. **B-C**: 67% and 33% 2D kernel density contours of species sharing the same habitat on the morphospace (**B**: PC1 against PC2, **C**: PC4 against PC5). **D:** Heatmaps showing the prediction accuracy of random forest models for each habitat based on two or seven morphospace axes. Predicted habitat states are displayed on the x axis and observed habitat states on the y axis. **E**: Mean accuracy of the random forest model at predicting habitat use based on the number of morphospace axes provided.

**Habitat transitions are associated with parallel shifts towards the same morphospatial regions.** We used a series of complementary process- and pattern-based approaches to quantitatively assess the strength of morphological convergence between lineages

285 independently transitioning towards the same habitat use category (thereafter called
286 "convergent lineages"). First, we compared the relative fit of a set of multivariate models of
287 trait evolution [mvMORPH, (54)] and found support for the multi-regime Brownian motion
288 model (BMMm), with distinct regimes corresponding to the five different habitat use categories
289 (i.e., habitat-dependent trait mean and evolutionary rate; Table S4). Thus, habitat use appears
290 to affect morphological evolution but categories did not correspond to unique optima (i.e.,
291 specific and restricted morphospatial regions), as BMM models do not model attraction toward
292 optima (in contrast with Ornstein–Uhlenbeck (OU) models, which provided worse fits of our
293 data (Table S4)).

294 We then assessed the phenotypic similarity between convergent taxa and distinctiveness
295 from other taxa [Wheatsheaf index (*w*), (55, 56)] and the increase in similarity between the
296 convergent taxa through time [C1 to C4 metrics (C-metrics), (10)]. *w* identified significantly
297 stronger convergence for lineages that independently transitioned to resting on the
298 ground/trunks, to resting on or hanging from branches, and to hanging from grass than would
299 be expected from a random distribution of trait values simulated under a Brownian Motion
300 (BM) model ($P < 0.04$, Table S5-6). Likewise, most of the C1 to C4 statistics were higher than
301 expected under random evolution for all habitats except lineages secondarily transitioning back
302 to hanging from branches (Table S5-6).

303 The C-metrics rely on the difference between the contemporary distance on the
304 morphospace between two convergent lineages ($D_{tip}$) and the maximum distance attained
305 between any two points (not necessarily synchronous) along the evolutionary trajectories of the
306 two lineages ($D_{max}$, Fig. 6C). Consequently, these metrics can be equally high for lineages that
307 had very dissimilar ancestors at some point in time but then subsequently became more similar,
308 and for lineages shifting in parallel towards a similar region of the morphospace (57). To
309 distinguish between these two scenarios, we computed the recently developed $C_t$ measures,

which compare the extant phenotypic distance between the convergent lineages to the maximum reconstructed ancestral distance at a given time point during their evolution (i.e., between synchronous points along the evolutionary trajectories) (57). Unlike C-metrics, $C_t$-metrics are only expected to be high when lineages diverged morphologically from one another at some point in their evolutionary history and then subsequently got closer (i.e., converged). $C_t$ measures were only significantly higher than expected by chance for transitions to resting on the leaf litter or trunks (Table S5-6). But even in this case, $C_t$ values were relatively close to zero, indicating that convergent taxa are not necessarily morphologically closer to one another than their ancestors. This suggests that lineages independently evolving similar habitat uses shifted in parallel towards the same broad region of the morphospace, and sometimes even diverged in that novel region (i.e., "imperfect" convergence (58)) (Fig. 6A-B). Parallelism (or collinearity (5)) was further confirmed by calculating the pairwise angles between the evolutionary trajectories on the morphospace of convergent lineages following the independent invasion of a given habitat ($\theta$, Fig. 6C)(28, 59, 60). $\theta$ was lower than expected by chance – indicating parallel evolutionary trajectories – for all habitat transitions except one, secondary transitions to hanging from branches (Table S5-6).

Convergence metrics were generally lower when not controlling for size to build the morphospace (Table S7), highlighting that convergence in habitat use is mainly associated with convergence in body shape, not size.

**Environmental similarity and phylogenetic relatedness promote stronger morphological convergence.** Whether two lineages evolve toward close or distant morphospatial regions following a similar habitat use transition may be affected by several factors including whether they started from the same ancestral habitat, the extent of environmental similarities between their new habitats, and their phylogenetic relatedness. We capitalized on the prolific repeated

independent habitat transitions in our study (toward resting on the leaf litter and trunks, n=16, Fig. 6A; and towards resting on branches and leaves, n=16, Fig. 6B) to quantify the relative importance of ancestral habitat similarity, environmental distance between derived habitats and time since divergence, on the strength of morphological convergence (the other habitat transitions were too rare to allow sufficient statistical power ($n \leq 4$, Fig. 5A)). We calculated pairwise environmental distances between convergent lineages as the distance on a multidimensional environmental space built from various macroecological variables relating to habitat height, climatic conditions, plant productivity and predator diversity (Fig. S12). For each pair of convergent lineages, we also scored whether they transitioned from the same habitat category or not (binary) and their divergence time as the age of their most recent common ancestor. Convergence between pairs of lineages was quantified as pairwise $D_{tip}$, $D_{max}$, $C_1$ and $\theta$ (Fig. 6C).

For both types of habitat use transition, multiple matrix regressions revealed that environmentally closer lineages (i.e., lineages colonizing more similar selective environments) and more closely related lineages transitioned toward closer positions on the morphospace (i.e., lower $D_{tip}$; Fig. 6D-E, Table S8). $D_{max}$ was only significantly affected by divergence time between the lineages: lineages that diverged a long time ago were more likely to exhibit a large $D_{max}$ relative to more closely related ones (Fig. 6F-G, Table S8). Consequently, $C_1$ decreased with environmental distance indicating weaker convergence between lineages experiencing more dissimilar environmental conditions (Fig. 6H, Table S8), and was only weakly affected by divergence time (Fig. 6I, Table S8). $\theta$ was primarily affected by divergence time: more closely related species pairs tended to follow more parallel evolutionary trajectories (Fig. 6J-K, Table S8). Lineages that transitioned toward the same habitat use category from different ancestral categories and thus potentially starting from further apart on the morphospace exhibited less parallel trajectories. However, this effect was only significant for the repeated

transitions to resting on branches and leaves (Table S8). These patterns were largely similar when using coordinates from a PCA controlling for phylogenetic covariance but excluding the two categorical variables on body texture (Table S9). However, they were not recovered when using coordinates from a PCA not controlling for size (Table S10) as habitat use appears to mainly drive convergence in body shape but not in body size.

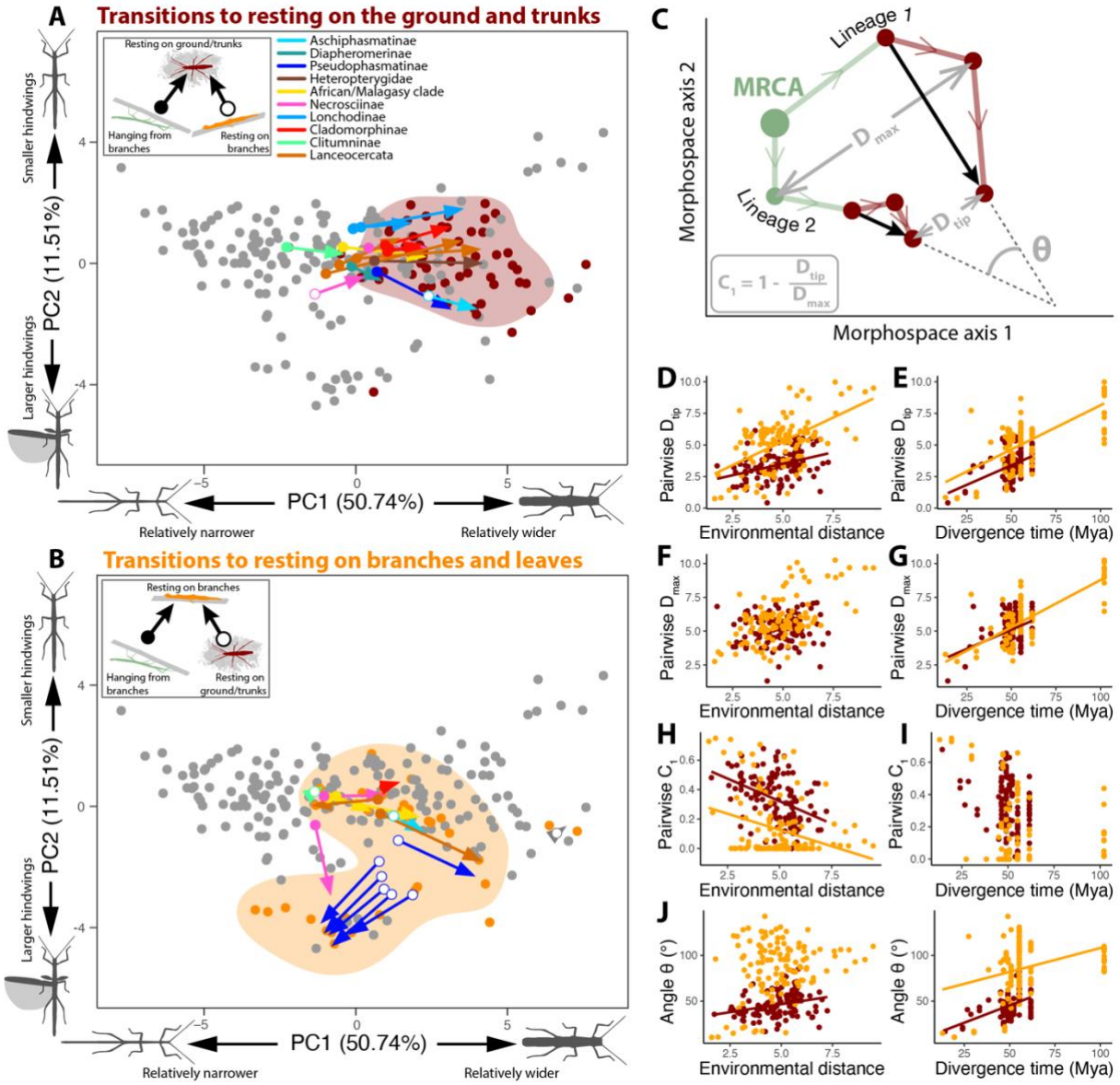


**Figure 6: Evolutionary trajectories and effects of environmental distance and divergence time on morphological convergence. A-B:** Trajectories on the morphospace of lineages that independently transitioned to resting on the ground and trunks (maroon, **A**) or to resting on branches and leaves (orange, **B**). Corresponding 75% 2D kernel density contours are shown. Arrows start at the inferred position of the ancestor that first transitioned to the new habitat. Arrows end at the centroid position of descendant species. Arrow colors correspond to genetic clades (see Fig.1). Start symbols indicate the ancestral habitat from which each lineage transitioned according to the insets. **C.** Example of the calculation of measures of convergence. The independent trajectories over time of two lineages splitting from their Most Recent Common Ancestor (MRCA) are shown on a

morphospace. These lineages start as hanging from branches (pale green) and independently transition to resting on the ground and trunks (maroon). Circles represent ancestral nodes or tips. $D_{tip}$ shows the current morphological distance between the two tips of interest. $D_{max}$ shows the maximum distance between the lineages at any point in time between the tips and the MRCA. $C_1$ calculates the proportion of the maximum distance between two lineages that has been erased by convergent evolution ($0 \leq C_1 \leq 1$). $\theta$ represents the angle between the two vectors starting from the first nodes in the new habitat state and ending at the tips. It compares the overall direction of change between lineages after independently invading the same habitat. **D-K**: Pairwise $D_{tip}$ (**D-E**), pairwise $D_{max}$ (**F-G**), pairwise $C_1$ (**H-I**) and pairwise $\theta$ (**J-K**) as a function of pairwise environmental distance and pairwise divergence time for each independent transitions to resting on the ground and trunks (maroon) and resting on branches and leaves (orange). Linear regressions are only shown if the effect of environmental distance and divergence time on the response variable are significant (see Table S8).

# Discussion

When adapting to shared environmental challenges, lineages often vary in the extent to which they evolve similar traits, indicating that evolutionary outcomes are more predictable in some instances than in others. Explaining this variation will be critical as scientists increasingly base medical (vaccine design, pandemic preparedness, antibiotic resistance, cancer therapies), agricultural (application of herbicides and pesticides, anticipating crop responses to climate change), and conservation (wildlife responses to anthropogenic disturbance and climate change) practices on predicted evolutionary responses to selection (61, 62). Here we used the dozens of instances of repeated habitat use transition in stick and leaf insects to quantify the relative contributions of divergence time (phylogenetic relatedness), similarity of most recent ancestral habitat, and the similarity of invaded environments, to the repeatability – and therefore the predictability – of phenotypic evolution. As in earlier studies of repeated evolution, we show that closely related lineages (i.e., likely sharing more genetic variation) followed more parallel evolutionary trajectories and ended up relatively closer on the morphospace, consistent with the idea that in the absence of opportunity for contingency, phenotypic responses to selection will be highly predictable (28, 63). Our study encompassed a wide range of divergence times (10 to 100 million years) and a large number of repeated habitat use transitions, permitting us to also show that the strength of morphological convergence decreases steadily with time since divergence (Fig. 6D-K, Table S8). Ironically, this suggests that for morphological evolution

even the stochastic contributions of contingency are predictable, in the sense that they accrue at a rather constant rate over time.

Classic examples of morphological convergence are often found among closely related taxa (e.g., *Anolis* lizards (16, 17), stickleback fish (18), cichlid fish (45)), suggesting that the repeatability of phenotypic evolution increases with relatedness (11). Closely related lineages appear predisposed to adapt in more similar ways when confronted with similar challenges, consistent with Gould's idea that evolution is less inclined to repeat itself at large macroevolutionary time scales (19). Here we provide an original and direct test of this idea in a system spanning vast divergence times (10 to 100 million years) (37, 41). In phasmids Gould's pattern was manifest in two ways: more closely related lineages responding independently to similar environmental challenges ended up looking more similar (i.e., more extensive convergence), and they followed more parallel paths on the morphospace to arrive there, than more distantly related lineage pairs. Closely related lineages likely share more standing genetic variation, and segregating variants are expressed against more similar genetic backgrounds (23, 64–66); and they are more likely to reuse the same genes when they adapt to similar environmental challenges (24–27).

The other factor influencing the strength of convergence is the environment: the more similar the selective conditions experienced by two lineages, the closer the resulting convergent phenotypes. Studies of phenotypic convergence often categorize ecological niches to identify associations between patterns of morphological evolution and the repeated adaptation to these discrete niches (e.g., diet types (58), lakes/streams (7, 13)). This categorization hides potential heterogeneities in environmental conditions among instances of the same category. Conditions that appear similar to a human observer may actually be disparate to the organisms, and this can confound studies attempting to explain variation in the strength of convergence. For example, stickleback fish independently colonizing stream habitats varied in the extent of their

phenotypic convergence in part because habitats categorized as "stream" actually differed in water clarity, temperature, parasite abundance, and food availability (28). Once these additional variables had been included, habitat similarity predicted the resulting strength of convergence more accurately (28).

Here we quantified niche similarity using various macro-ecological variables, and our results suggest that some of the niches invaded by phasmids (e.g., grass) were largely uniform and thus likely experienced very similarly across lineages, while others (e.g., resting on branches and leaves) encompassed much wider and potentially less similar environmental conditions (i.e., they likely included "cryptic" dissimilarities between habitat use categories) (Fig. S13). We show that environmental similarity of invaded habitats also predicted strength of convergence: lineages switching to more similar environments within a given habitat use category ended up in closer regions of the morphospace (Fig. 6D,H), even across large macroevolutionary time scales and despite the higher associated opportunities for contingency.

Finally, we accounted for similarity of the most recent *ancestral* habitats of convergent pairs of lineages, to test whether transitioning from the same or different habitat categories affected the extent of the resulting convergence in this group of insects. Lineages that transitioned toward the same habitat *from the same ancestral habitat* tended to follow more parallel or collinear trajectories, but this effect was only significant for transitions to resting on branches and leaves (Table S8). It is possible that there were not enough transitions from the same versus different ancestral habitats for transitions to resting on trunks and leaf litter to detect this effect.

The Euphasmatodea show a deep radiation at the base of the group (~65–55Mya) following the K-T boundary (37), corresponding with the origin of most major clades and with dispersal across vast regions of the globe (Fig. 2). Although a few of these clades seem to have undergone speciation without niche differentiation, and species within these clades are

457 morphologically homogeneous (e.g., Phylliidae (wide leaf mimics and canopy-dwellers) and
458 the Heteropterygidae (spiny and robust ground-dwellers), which are distributed on many islands
459 of Indomalaya and Australasia (Fig. 3C, 5A, S11) (44, 67)), the majority of euphasmatodean
460 clades subsequently radiated into multiple different ecomorphs colonizing diverse habitats (e.g.,
461 Lanceocercata (Australasia and Mascarene islands), Cladomorphinae (Caribbean islands),
462 Lonchodinae (Indomalaya/ Australasia), Necrosciinae (Indomalaya), African/Malagasy clade
463 (Afrotropics), Pseudophasmatinae (Neartic and Neotropics) and Diapheromerinae (Neartic and
464 Neotropics); Fig. 3C, 5A, S11) (35, 44, 67, 68). We characterized 21 different phasmid
465 ecomorphs and reconstructed dozens of evolutionary transitions between ecological niches,
466 resulting in repeated instances of convergence towards these phasmid body forms. Overall, our
467 results suggest the extremely diverse morphologies of stick and leaf insects result from
468 replicated radiations in different geographic regions, each associated with widespread parallel
469 shifts on the morphospace as independent lineages adapted to similar habitats.
470

# Conclusion

Stick and leaf insects exemplify the extraordinary power of natural selection to shape organismal phenotypes. The animals themselves are charismatic champions of crypsis and masquerade, and our comprehensive quantification of their trajectories of morphological evolution, using process-based (i.e., evolutionary modelling) and pattern-based methods, reveals dozens of instances of convergence. We show that the details of the environmental conditions experienced by the organisms – the closeness of the invaded niches and the similarity of their starting, or ancestral, niche – predict the extent of convergence even when the lineages in question have been evolving independently for tens of millions of years, and therefore have had ample opportunity for contingency. Furthermore, we show that even the effects of contingency are predictable, eroding the strength of convergence at a gradual and steady rate across vast spans of time. We suggest that precise quantification of selective environments, as well as divergence times, will be critical as studies increasingly attempt to predict the outcomes of evolution.

# Materials and Methods

Extended materials and methods are reported in the SI Appendix, Supplementary Materials and Methods, and include details on definitions and choices of convergence metrics.

**Taxonomic sampling and phylogenetic reconstruction.** Well-supported phylogenies for 38 phasmid lineages representing all major clades of Phasmatodea were recently reconstructed using next-generation sequencing (transcriptomes), yielding topologies that resolved most of the deep nodes within this group with high confidence (37, 41). Here we reconstructed a phylogeny with 314 species representing all major phasmid lineages (9% of the known phasmid species diversity and 33% of currently recognized generic diversity), and one species of Embioptera (the sister clade of Phasmatodea) as outgroup, constraining the basal topology to match the transcriptome-based trees (41). Regions of 3 nuclear (18S rRNA (18S), 28S rRNA (28S) and histone subunit 3 (H3)) and 4 mitochondrial genes (12S rRNA (12S), 16S rRNA (16S), cytochrome-c oxidase subunit I (COI) and cytochrome-c oxidase subunit II (COII)) were extracted from Genbank, aligned and concatenated (6,778bp total) to reconstruct a Maximum Clade Credibility (MCC) tree for phasmids using Bayesian inferences in BEAST 2 (v. 2.6.3)(dataset S1) (69). Divergence time was estimated using 6 unambiguous crown-group phasmid fossils as minimum calibration points (Table S1).

**Morphological data.** We examined 1359 adult female specimens from 212 species included in the phylogeny. High-quality photographs, captured in dorsal and/or lateral views, were obtained from our own collection at the University of Göttingen (Germany), other museum collections, the published literature and other online sources (dataset S1). Depending on material availability, we measured pictures of between 1 and 18 different individuals per species (mean = 5.5 individuals per species). We collected 21 continuous measurements (Fig. S1) that together contained biologically relevant information about overall body size and shape, width and length of different body segments (notably the head), leg length, hindwing size and the length of the

512 subgenital plate (whose function is often related to oviposition). We also qualitatively scored
513 the texture of the mesothorax and abdomen (1: spiny/rough, 0: smooth). Body volume was used
514 as a proxy for body size and was calculated as the volume of an elliptical cylinder of the same
515 length, average width and height as the body of the insect (Fig. S1).
516 **The phasmid morphospace.** We built a multidimensional morphospace using a Principal
517 Component Analysis (PCA) mixing continuous and categorical data ($PCA_{mix}$) (43). To avoid
518 differences in body size (which can vary by as much as three hundred-fold in volume)
519 dominating differences in body shape and to remove allometric effects, we size-corrected the
520 continuous measurements (6, 13, 70). We substituted original measurement values with the
521 residuals calculated from a phylogenetically-corrected linear regression against body volume
522 (R package "phytools") (51, 71), after $log_{10}$-transformation. Because wing length and wing area
523 included zeros for wingless species, we divided the non-transformed measurements by body
524 length or body length squared respectively, to obtain and include measures of relative wing
525 length and area. In total, we included 21 continuous (previously mean-centered on zero and
526 scaled to unit variance) and two categorical variables (Fig. S1-2). To make sure that categorical
527 variables and size correction were not biasing our results, we also ran PCA analyses including
528 a phylogenetic correction and excluding the two categorical variables. The continuous variables
529 were either corrected for size ($pPCA_c$) or not ($pPCA_{nc}$) (see supplementary methods, Fig. S14-
530 15).
531 **Habitat data.** We broadly classified the habitat use of stick insects based on the typical resting
532 posture and substrate preferences exhibited by adult females when hiding during the day (i.e.,
533 when they are exposed to visually hunting predators). We surveyed the literature, field guides
534 and iNaturalist (https://www.inaturalist.org/, accessed July 2021) for observations of where
535 each species is typically found (dataset S1). We defined five habitat use categories: resting on
536 the ground or trunks (including the base of trunks, mossy logs, under bark, in the leaf litter),

resting on branches and leaves, hanging from branches and leaves, hanging from grass, and resting on palm leaves. We acknowledge that this classification is broad and consequently does not fully encompass the entire spectrum of substrates and host plants upon which phasmids may be found (32–34).

**Environmental data.** We gathered information about the geographic range of each species based on sampling location of type specimens and observations on iNaturalist (available from https://www.inaturalist.org, accessed July 2021). For each species, we then selected the median location with the most central latitude. From the GPS coordinates of the most central location for each species, we extracted data on 17 environmental variables that together contained information about climatic conditions (temperature, precipitation, seasonality), vegetation density and food availability (primary production), predator diversity and habitat vegetation layer (see Supplementary information, dataset S1). Variation in these variables was summarized by running a principal component analysis (Fig. S12).

**Definition of ecomorphs.** We used our multidimensional morphospace data ($PCA_{mix}$) to cluster species into distinct ecomorphs by running a hierarchical clustering algorithm (using the Ward's method) to define ecomorphs based on overall proximity on the morphospace (defined by the first 7 PC axes, accounting for 90% of the total variation). We defined the optimal number of clusters using the Biological Homogeneity Index (BHI), which measured how homogeneous clusters are, based on habitat use (R package "clValid") (46, 72). Clusters were defined by a fixed height threshold on the clustering dendrogram. The optimal number of clusters was then chosen to minimize the number of clusters while maximizing BHI (i.e., start of a plateau, Fig. S6). We then identified the morphospace axes that best distinguished each ecomorph by training random forest models (R package "randomForest") (48) to classify a taxon in either an ecomorph of interest or in a different one, given the first seven axes of the $PCA_{mix}$ morphospace (Table S3).

**Overlap between habitat categories on the morphospace.** To quantify morphospace occupation by species exhibiting different habitat uses (Fig. 5B-C), we estimated multidimensional hypervolumes using dynamic range boxes (R package "dynRB")(52) and high-dimensional kernel density estimations (R package “hypervolume”)(53), including either PC1-PC7 of $PCA_{mix}$ (90.1% of the total variation), PC1-PC8 of $pPCA_{nc}$ (91.5%) or PC1-PC6 of $pPCA_{c}$ (92.1%)(Fig. S7-8). Pairwise hypervolume overlap was quantified for the $PCA_{mix}$ morphospace as the portion of the hypervolume of habitat A covered by the hypervolume of habitat B and vice versa, as the Jaccard similarity index (ratio of the intersection to the union of the hypervolumes), or as the Sørensen–Dice similarity index (ratio of twice the size of the intersection to the sum of the individual hypervolumes) (Fig. S9-10). The distance between the hypervolumes was also quantified as the Euclidean distance between the hypervolume centroids and the minimum Euclidean distance between points of the two hypervolumes (Fig. S10). Finally, we also quantified the overlap between the habitat categories on the $PCA_{mix}$ morphospace using machine learning random forest models (48). These models were used to predict the habitat category of a species given its position on the morphospace. The predictive error rate of the models was used to quantify overlap between habitat categories (Fig. 5D-E).

**Ancestral state reconstruction of ecomorphs and habitat use.** Habitat use was mapped on the MCC tree to uncover the number of independent transitions toward each of the five categories (Fig. 5A). We ran ancestral state reconstructions using stochastic character mapping as implemented in the R package “phytools” (51). The transition matrix was calculated using maximum likelihood and using an all-rates-different model (model= “ARD”). Ecomorphs, as defined by our hierarchical clustering analysis, were similarly mapped to establish whether they had single or multiple origins (Fig. 3C). Given the large number of ecomorphs (n=21), only the “equal rate” transition model (assuming a single transition rate between ecomorphs) could be run.

**Process-based tests of convergence – evolutionary model fitting.** To test for morphological convergence among lineages that independently transitioned to the same habitat, we fitted multivariate models of continuous trait evolution to PC1-PC5 ($PCA_{mix}$, 84% of the total variance) using the "mvMORPH" R package (54). We first fit the single-regime Brownian motion (BM1, modeling stochastic trait changes over time), Ornstein–Uhlenbeck (OU1, modeling attraction towards an optimal trait value), and early burst models (EB, modeling stochastic changes with a decrease in evolutionary rate over time), which represent the null hypotheses. Then, for each habitat category, we fit 2-regime models where the given habitat category was considered its own evolutionary regime while the rest belonged to another unique regime. We also ran 5-regime models including each habitat as a separate regime. The ancestral histories for each of the tested regime assignments were reconstructed on the MCC tree using 100 stochastic character maps (51). We fitted multi-regime OU models (OUM) allowing trait optima to vary among regimes, and BM models allowing on one hand the phylogenetic means to vary among regimes, and on the other hand holding the evolutionary rate constant (BM1m) or not (BMMm).

**Pattern-based tests of convergence.** To quantify the strength of morphological convergence associated with repeated habitat transitions, we calculated the C1 to C4 pattern-based metrics (R package "convevol")(10) as well as the Wheatsheaf index ($w$) ("windex") (55, 56) for PC1-PC7 of $PCA_{mix}$ (90.1% of the total variation), PC1-PC8 of $pPCA_{nc}$ (91.5%) and PC1-PC6 of $pPCA_{c}$ (92.1%). $C_1$-$C_4$ are based on the ratio between the current distance between two lineages ($D_{tip}$) on the morphospace to the maximum reconstructed distance between the two lineages at any point in the past ($D_{max}$) (Fig. 6C). $C_1$-$C_4$ will be high when independent lineages diverged substantially after splitting and then subsequently re-evolved similarities, or when convergent lineages shifted in parallel towards the same direction on the morphospace (57). To distinguish between these two scenarios, we computed the recently developed $Ct_1$-$Ct_4$ metrics, which

restrict $D_{max}$ to synchronous nodes (57). $Ct_1$-$Ct_4$ are only expected to be high in the first scenario (divergence first, then convergence). Finally, we quantified parallelism in the evolutionary trajectories of convergent lineages by calculating the angle ($\theta$) between these trajectories on the morphospace (59, 60, 73). We reconstructed the trajectories of convergent lineages from the position of the node immediately prior to the inferred habitat transition, to that of the tip of interest (Fig. 6C). For each above-described variable, p-values were inferred following 1000 simulations of random character evolution, testing the hypothesis that convergence is significantly stronger (or that trajectories are more parallel) in the habitat category of interest than would be expected by chance.

**Explaining variation in the extent of morphological convergence.** We tested the effects of three factors on the extent of morphological convergence: the phylogenetic relatedness between the convergent lineages, their environmental similarity, and whether they started from the same ancestral habitat use category. We only considered the repeated transitions toward resting on the leaf litter and trunks (n=16, Fig. 6A) and towards resting on branches and leaves (n=16, Fig. 6B) for these analyses as other transitions were too rare to allow sufficient statistical power ($n \leq 4$, Fig. 5A). For each transition type, phylogenetic relatedness, environmental distance, ancestral habitat difference and morphological convergence were computed for all possible pairs of taxa corresponding to separate independent transitions toward the habitat category, and then assembled as distance matrices. Pairwise phylogenetic relatedness was estimated as the age of the most recent common ancestor of the two lineages. Pairwise environmental distance was calculated as the Euclidean distance on the environmental PC1-PC7 (accounting for 90% of the total environmental variation). Pairwise ancestral habitat difference was scored as either 0 if both lineages transitioned to the habitat of interest from the same ancestral habitat, or 1 otherwise. Finally, to quantify morphological convergence we computed pairwise $D_{tip}$, pairwise $D_{max}$, pairwise $C_1$ and pairwise $\theta$ using PC1-PC7 of $PCA_{mix}$ (90.1% of the total variation), PC1-

PC8 of $pPCA_{nc}$ (91.5%) or PC1-PC6 of $pPCA_{c}$ (92.1%). We fitted multiple matrix regressions (partial Mantel tests, R package "phytools") with 100,000 Mantel permutations to compute P-values. Phylogenetic relatedness, environmental distance and ancestral habitat difference were included as explanatory variables, and either $D_{tip}$, $D_{max}$, $C_1$ or $\theta$ as response variables. The choice of variables to compare the magnitude of convergence across independent habitat transitions is extensively discussed in the supplementary information. Finally, we verified the robustness of the recovered patterns to the independent habitat transitions we included by bootstrap sampling the two types of independent transitions 100 times, and checking the consistency of the effects of the three explanatory variables on the different response variables.

# Acknowledgments

We thank Camille Thomas-Bulle, Tanja Schwander, Anthony Lapsansky, Guillaume Lavanchy and William Toubiana for insightful discussions on the manuscript. This study would not have been possible without the work of many passionate phasmid enthusiasts and breeders who, over the years, documented the biology of many species. We are therefore very grateful to the amateur and professional phasmid community for publicly or privately sharing these notes and observations along with many high quality pictures. We are thankful to Nicolas Cliquennois for insightful discussions regarding Malagasy and Mascarene stick insects. We thank Paul Bertner, Angus McNab, Chien C. Lee, Bruno Kneubühler, Nicolas Cliquennois and Paul Brock for permission to use their pictures. Finally, we thank Jonathan B. Losos and Scott V. Edwards for for reviews that substantially improved this manuscript.

This research was supported by NSF IOS-2015907 to DJE.

## References


1. S. Conway Morris, *The runes of evolution: how the universe became self-aware* (Templeton Press, 2015).
2. G. R. McGhee, *Convergent evolution: limited forms most beautiful* (MIT Press, 2011).
3. J. B. Losos, Convergence, adaptation, and constraint. *Evolution* **65**, 1827–1840 (2011).
4. D. B. Wake, M. H. Wake, C. D. Specht, Homoplasy: From detecting pattern to determining process and mechanism of evolution. *Science* **331**, 1032–1035 (2011).
5. J. Cerca, Understanding natural selection and similarity: Convergent, parallel and repeated evolution. *Molecular Ecology* **32**, 5451–5462 (2023).
6. D. M. Grossnickle, *et al.*, Incomplete convergence of gliding mammal skeletons. *Evolution* **74**, 2662–2680 (2020).
7. P. Trontelj, A. Blejec, C. Fišer, Ecomorphological convergence of cave communities. *Evolution* **66**, 3852–3865 (2012).
8. Š. Borko, P. Trontelj, O. Seehausen, A. Moškrič, C. Fišer, A subterranean adaptive radiation of amphipods in Europe. *Nature Communications* **12**, 1–12 (2021).
9. R. G. Gillespie, S. P. Benjamin, M. S. Brewer, M. A. J. Rivera, G. K. Roderick, Repeated diversification of ecomorphs in hawaiian stick spiders. *Current Biology* **28**, 941–947 (2018).
10. C. T. Stayton, The definition, recognition, and interpretation of convergent evolution, and two new measures for quantifying and assessing the significance of convergence. *Evolution* **69**, 2140–2153 (2015).
11. T. J. Ord, T. C. Summers, Repeated evolution and the impact of evolutionary history on adaptation. *BMC Evolutionary Biology* **15**, 1–12 (2015).
12. C. T. Stayton, Is convergence surprising? An examination of the frequency of convergence in simulated datasets. *Journal of Theoretical Biology* **252**, 1–14 (2008).
13. D. Esquerré, J. Scott Keogh, Parallel selective pressures drive convergent diversification of phenotypes in pythons and boas. *Ecology Letters* **19**, 800–809 (2016).
14. Z. D. Blount, R. E. Lenski, J. B. Losos, Contingency and determinism in evolution: Replaying life's tape. *Science* **362**, eaam5979 (2018).
15. A. A. Agrawal, Toward a predictive framework for convergent evolution: Integrating natural history, genetic mechanisms, and consequences for the diversity of life. *American Naturalist* **190**, S1–S12 (2017).
16. J. B. Losos, T. R. Jackman, A. Larson, K. De Queiroz, L. Rodríguez-Schettino, Contingency and determinism in replicated adaptive radiations of island lizards. *Science* **279**, 2115–2118 (1998).
17. L. D. Mahler, T. Ingram, L. J. Revell, J. B. Losos, Exceptional Convergence on the Macroevolutionary Landscape in Island Lizard Radiations. *Science* **341**, 292–295 (2013).
18. P. F. Colosimo, *et al.*, Widespread parallel evolution in sticklebacks by repeated fixation of ectodysplasin alleles. *Science* **307**, 1928–1933 (2005).
19. S. J. Gould, *Wonderful life: the Burgess Shale and the nature of history.* (W. W. Norton & Company, 1989).
20. S. J. Gould, *The structure of evolutionary theory.* (Harvard University Press, 2002).
21. V. Orgogozo, Replaying the tape of life in the twenty-first century. *Interface Focus* **5**, 20150057 (2015).
22. R. D. H. Barrett, S. M. Rogers, D. Schluter, Natural selection on a major armor gene in threespine stickleback. *Science* **322**, 255–7 (2008).
23. G. L. Conte, M. E. Arnegard, C. L. Peichel, D. Schluter, The probability of genetic parallelism and convergence in natural populations. *Proceedings of the Royal Society B: Biological Sciences* **279**, 5039–5047 (2012).

24. M. Bohutínská, *et al.*, Genomic basis of parallel adaptation varies with divergence in Arabidopsis and its relatives. *Proceedings of the National Academy of Sciences of the United States of America* **118**, e2022713118 (2021).
25. S. Chaturvedi, *et al.*, Climatic similarity and genomic background shape the extent of parallel adaptation in Timema stick insects. *Nature Ecology & Evolution* **6**, 1952–1964 (2022).
26. G. Montejo-Kovacevich, *et al.*, Repeated genetic adaptation to altitude in two tropical butterflies. *Nature Communications* **13**, 1–16 (2022).
27. I. S. Magalhaes, *et al.*, Intercontinental genomic parallelism in multiple three-spined stickleback adaptive radiations. *Nature Ecology & Evolution* **5**, 251–261 (2021).
28. Y. E. Stuart, *et al.*, Contrasting effects of environment and genetics generate a continuum of parallel evolution. *Nature Ecology and Evolution* **1**, 1–7 (2017).
29. M. Bohutínská, C. L. Peichel, Divergence time shapes gene reuse during repeated adaptation. *Trends in Ecology & Evolution* **39**, 396–407 (2024).
30. G. D. Ruxton, W. L. Allen, T. N. Sherratt, M. P. Speed, *Avoiding attack: the evolutionary ecology of crypsis, aposematism, and mimicry.* (Oxford University Press, 2019).
31. J. Skelhorn, H. M. Rowland, M. P. Speed, G. D. Ruxton, Masquerade: camouflage without crypsis. *Science* **327**, 51 (2010).
32. G. O. Bedford, Biology and ecology of the Phasmatodea. *Annual Review of Entomology* **23**, 125–149 (1978).
33. S. Bradler, T. R. Buckley, "Biodiversity of Phasmatodea" in *Insect Biodiversity: Science and Society*, R. G. Foottit, P. H. Adler, Eds. (Wiley-Blackwell, 2018), pp. 281–313.
34. P. D. Brock, T. H. Büscher, *Stick and Leaf-Insects of the World* (NAP Editions, 2022).
35. T. R. Buckley, D. Attanayake, S. Bradler, Extreme convergence in stick insect evolution: phylogenetic placement of the Lord Howe Island tree lobster. *Proceedings of the Royal Society B: Biological Sciences* **276**, 1055–1062 (2009).
36. S. Bradler, N. Cliquennois, T. R. Buckley, Single origin of the Mascarene stick insects: ancient radiation on sunken islands? *BMC Evolutionary Biology* **15**, 1–10 (2015).
37. S. Simon, *et al.*, Old world and new world Phasmatodea: phylogenomics resolve the evolutionary history of stick and leaf insects. *Frontiers in Ecology and Evolution* **7**, 1–14 (2019).
38. S. Bradler, J. A. Robertson, M. F. Whiting, A molecular phylogeny of Phasmatodea with emphasis on Necrosciinae, the most species-rich subfamily of stick insects. *Systematic Entomology* **39**, 205–222 (2014).
39. J. A. Robertson, S. Bradler, M. F. Whiting, Evolution of oviposition techniques in stick and leaf insects (Phasmatodea). *Frontiers in Ecology and Evolution* **6**, 1–15 (2018).
40. N. Cliquennois, Révision des Anisacanthidae, famille endémique de phasmes de Madagascar (Phasmatodea: Bacilloidea). *Annales de la Societe Entomologique de France* **44**, 59–85 (2008).
41. E. Tihelka, C. Cai, M. Giacomelli, D. Pisani, P. C. J. Donoghue, Integrated phylogenomic and fossil evidence of stick and leaf insects (Phasmatodea) reveal a Permian–Triassic co-origination with insectivores. *Royal Society Open Science* **7**, 201689 (2020).
42. S. Bank, S. Bradler, A second view on the evolution of flight in stick and leaf insects (Phasmatodea). *BMC Ecology and Evolution* **22**, 1–17 (2022).
43. M. Chavent, V. Kuentz-Simonet, A. Labenne, J. Saracco, Multivariate Analysis of Mixed Data: The R Package PCAmixdata. *arXiv* (2017).
44. S. Bank, *et al.*, A tree of leaves: phylogeny and historical biogeography of the leaf insects (Phasmatodea: Phylliidae). *Communications Biology* **4**, 1–12 (2021).
45. M. Muschick, A. Indermaur, W. Salzburger, Convergent Evolution within an Adaptive Radiation of Cichlid Fishes. *Current Biology* **22**, 2362–2368 (2012).

760 46. S. Datta, S. Datta, Methods for evaluating clustering algorithms for gene expression
761 data using a reference set of functional classes. *BMC Bioinformatics* **7**, 1–9 (2006).
762 47. E. E. Williams, "The Origin of Faunas. Evolution of Lizard Congeners in a Complex
763 Island Fauna: A Trial Analysis" in *Evolutionary Biology*, T. Dobzhansky, M. K. Hecht, W. C.
764 Steere, Eds. (Springer US, 1972), pp. 47–89.
765 48. A. Liaw, M. Wiener, Classification and regression by randomForest. *R News* **2**, 18–22
766 (2002).
767 49. J. P. Huelsenbeck, R. Nielsen, J. P. Bollback, Stochastic Mapping of Morphological
768 Characters. *Systematic Biology* **52**, 131–158 (2003).
769 50. J. P. Bollback, SIMMAP: Stochastic character mapping of discrete traits on
770 phylogenies. *BMC Bioinformatics* **7**, 88 (2006).
771 51. L. J. Revell, phytools: An R package for phylogenetic comparative biology (and other
772 things). *Methods in Ecology and Evolution* **3**, 217–223 (2012).
773 52. R. R. Junker, J. Kuppler, A. C. Bathke, M. L. Schreyer, W. Trutschnig, Dynamic
774 range boxes – a robust nonparametric approach to quantify size and overlap of n-dimensional
775 hypervolumes. *Methods in Ecology and Evolution* **7**, 1503–1513 (2016).
776 53. B. Blonder, *et al.*, hypervolume: high dimensional geometry, set operations,
777 projection, and inference using kernel density estimation, support vector machines, and
778 convex hulls. (2023). Deposited 2023.
779 54. J. Clavel, G. Escarguel, G. Merceron, mvmorph: an r package for fitting multivariate
780 evolutionary models to morphometric data. *Methods in Ecology and Evolution* **6**, 1311–1319
781 (2015).
782 55. K. Arbuckle, C. M. Bennett, M. P. Speed, A simple measure of the strength of
783 convergent evolution. *Methods in Ecology and Evolution* **5**, 685–693 (2014).
784 56. K. Arbuckle, A. Minter, Windex: Analyzing convergent evolution using the
785 wheatsheaf index in R. *Evolutionary Bioinformatics* **2015**, 11–14 (2015).
786 57. D. M. Grossnickle, *et al.*, Challenges And Advances In Measuring Phenotypic
787 Convergence. *Evolution* qpae081 (2024). https://doi.org/10.1093/evolut/qpae081.
788 58. D. C. Collar, J. S. Reece, M. E. Alfaro, P. C. Wainwright, R. S. Mehta, Imperfect
789 morphological convergence: Variable changes in cranial structures underlie transitions to
790 durophagy in moray eels. *American Naturalist* **183** (2014).
791 59. D. C. Adams, M. L. Collyer, A general framework for the analysis of phenotypic
792 trajectories in evolutionary studies. *Evolution* **63**, 1143–1154 (2009).
793 60. D. I. Bolnick, R. D. H. Barrett, K. B. Oke, D. J. Rennison, Y. E. Stuart, (Non)Parallel
794 evolution. *Annual Review of Ecology, Evolution, and Systematics* **49**, 303–330 (2018).
795 61. M. Lässig, V. Mustonen, A. M. Walczak, Predicting evolution. *Nature Ecology &*
796 *Evolution* **1**, 1–9 (2017).
797 62. M. T. Wortel, *et al.*, Towards evolutionary predictions: Current promises and
798 challenges. *Evolutionary Applications* **16**, 3–21 (2023).
799 63. T. Leinonen, R. J. S. McCairns, G. Herczeg, J. Merilä, Multiple evolutionary pathways
800 to decreased lateral plate coverage in freshwater threespine sticklebacks. *Evolution* **66**, 3866–
801 3875 (2012).
802 64. E. B. Rosenblum, C. E. Parent, E. E. Brandt, The molecular basis of phenotypic
803 convergence. *Annual Review of Ecology, Evolution, and Systematics* **45**, 203–229 (2014).
804 65. J. F. Storz, Causes of molecular convergence and parallelism in protein evolution.
805 *Nature Reviews Genetics* **17**, 239–250 (2016).
806 66. A. J. Verster, A. K. Ramani, S. J. McKay, A. G. Fraser, Comparative RNAi screens in
807 C. elegans and C. briggsae reveal the impact of developmental system drift on gene function.
808 *PLOS Genetics* **10**, e1004077 (2014).
809 67. S. Bank, *et al.*, Reconstructing the nonadaptive radiation of an ancient lineage of

ground-dwelling stick insects (Phasmatodea: Heteropterygidae). *Systematic Entomology* **46**, 487–507 (2021).
68. Y. M. Pacheco, "Ecomorph Convergence in Stick Insects ( Phasmatodea ) with Emphasis on the Lonchodinae of Papua New Guinea," Brigham Young University. (2018).
69. R. Bouckaert, *et al.*, BEAST 2: A Software Platform for Bayesian Evolutionary Analysis. *PLOS Computational Biology* **10**, e1003537 (2014).
70. S. A. Price, *et al.*, Building a Body Shape Morphospace of Teleostean Fishes. *Integrative and Comparative Biology* **59**, 716–730 (2019).
71. L. J. Revell, Size-correction and principal components for interspecific comparative studies. *Evolution* **63**, 3258–3268 (2009).
72. G. Brock, V. Pihur, S. Datta, S. Datta, clValid: An R Package for Cluster Validation. *Journal of Statistical Software* **25**, 1–22 (2008).
73. D. C. Adams, M. L. Collyer, Phylogenetic Comparative Methods and the Evolution of Multivariate Phenotypes. *Annual Review of Ecology, Evolution, and Systematics* **50**, 405–425 (2019).